3

Structure and Reactivity of Solid Catalysts — Quantum Chemical Approach

Joachim Sauer

Institute of Chemistry, Humboldt University, Unter den Linden 6, 10117 Berlin, Germany

Abstract

Three different types of catalysts are considered. The first are zeolites which have a known crystal structure, the second are model catalysts used in ultra-high vacuum studies, and the third are supported transition metal oxides, for which the size and distribution of active particles is not known. For the proton forms of zeolites we study possible products of the protonation of isobutene as an example of hydrocarbon transformation. For model catalysts we describe how quantum mechanics and surface science successfully cooperate in determining the structure of an ultra-thin silica film on an Mo(110) substrate. Vanadium oxide on silica and alumina are chosen for studying the mechanism of methanol oxidation and oxidative dehydrogenation of propane. The dependence of the reactivity on the size of the active particles below monolayer coverage is analyzed and compared with the reactivity of crystalline V_2O_5.

1. INTRODUCTION

Quantum mechanics became an indispensable tool in catalysis research that is most powerful when applied in close collaboration with experimental techniques. Quantum mechanics is used to identify surface structures by assigning experimental signatures to structure models, to predict stabilities of different structure models depending on conditions (temperature, gas pressure such as oxygen and water), and to identify active species on supports. Quantum mechanics is unique in proposing or investigating reaction mechanisms by calculating energy and free energy profiles for catalytic reactions.

Understanding the structure and reactivity of solid supported transition metal oxide catalysts is facilitated by investigating less complex model systems such as gas phase clusters, deposited clusters, crystal surfaces and thin films under UHV

conditions. Quantum mechanics in combination with statistical mechanics is able to predict unusual structures and their stability as a function of external conditions (O_2 gas pressure and temperature) and composition. Structure determinations using diffraction methods are hardly possible and the most successful strategy is comparison of observed spectra (IR, Raman, XPS) and observed STM patterns with those obtained by quantum calculations for predicted structures. Examples are ultrathin SiO_2-films supported on Mo [1,2] and vanadium oxides supported on SiO_2 and Al_2O_3 [3].

2. HYDROCARBON REACTIONS IN ZEOLITES

The mechanisms of hydrocarbon transformation reactions using zeolite catalysts are not completely understood. In particular, the nature of intermediates formed on the interaction of alkenes with H-zeolites or by hydride abstraction from alkanes is still controversial. Specifically, it is not clear whether carbenium ions are intermediates or merely transition structures. Many experimental attempts have been made to identify the *tert*-butyl cation as intermediate. For isobutene in H-ferrierite we showed by DFT (periodic boundary conditions) that the hydrogen-bonded complex is most stable, while the isobutyl and *tert*-butyl alkoxides as well as the *tert*-butyl cation are possible intermediates [4].

The interaction of hydrocarbons with zeolite surfaces cannot be reliably described by DFT because currently used functionals do not account for dispersion in the region of non-overlapping charge densities. In contrast, MP2 is perfectly suited to do this, but cannot be applied with periodic boundary conditions and large unit cells. To solve this problem we use a hybrid MP2:DFT scheme [5] within a multilevel approach that yields an estimate of the MP2 reaction energy for the full periodic system. It includes extrapolation of the MP2 energy to the complete basis set limit as well as extrapolation of the high-level (MP2) correction to the limiting case of the full periodic structure. The latter is done by calculating the MP2 correction for a series of cluster models of increasing size, fitting an analytic expression to these energy corrections, and applying the fitted expression to the full periodic structure. We assume that, up to a constant, the high-level correction is described by a damped dispersion expression.

The hybrid MP2:DFT results in Figure 1 show that the stability of hydrocarbon species in zeolites is heavily underestimated by DFT(PBE) and that this underestimation is not uniform for different types of intermediates. In particular, the *tert*-butyl cation is significantly less stable (- 27 kJ/mol with respect to isobutene in the gas phase) than the neutral adsorption complex (-74 kJ/mol) or the isobutoxide (-63 kJ/mol) [6].

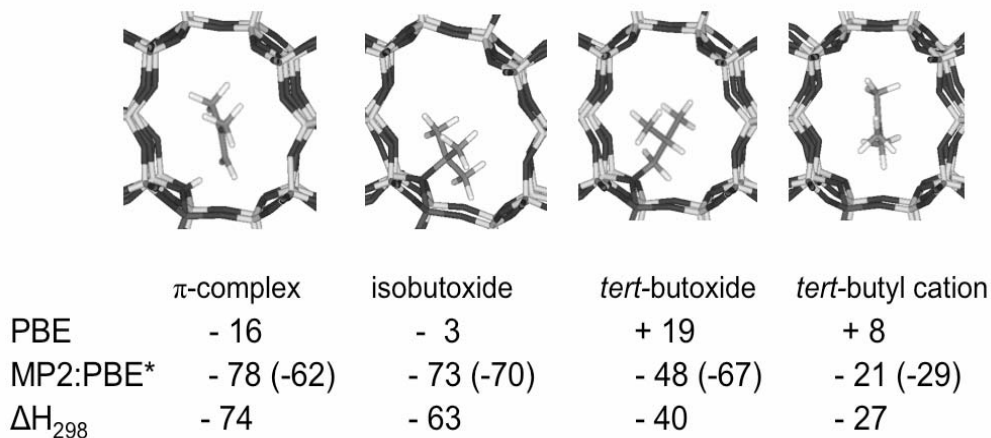|	π-complex	isobutoxide	tert-butoxide	tert-butyl cation
PBE	- 16	- 3	+ 19	+ 8
MP2:PBE*	- 78 (-62)	- 73 (-70)	- 48 (-67)	- 21 (-29)
ΔH_{298}	- 74	- 63	- 40	- 27

Figure 1. Different structures resulting from adsorption of isobutene in H-ferrierite as obtained by hybrid MP2:DFT calculations. Below the structures, the interaction energies with respect to H-FER and isobutene in the gas phase are given in kJ/mol. PBE refers to energies obtained by DFT calculations (PBE functional) and MP2:PBE refers to hybrid MP2:PBE calculations. The numbers in parenthesis are the changes from PBE. ΔH_{298} are heats of adsorption at 298 K calculated from MP2:PBE energies and frequencies obtained with PBE.

We conclude that DFT calculations with currently used functionals such as described in Ref. [7] are not suitable for treating catalytic hydrocarbon transformations in zeolites. Because of the large computational effort, the proposed hybrid MP2:PBE method is not routinely applicable, but will be very valuable in obtaining benchmark results for the much simpler DFT+damped dispersion approach [8].

3. THE STRUCTURE OF MODEL CATALYSTS

The first step in building a supported model catalyst is growing a thin ordered film of the supporting oxide on a metal substrate. For silica on Mo(112), LEED and STM showed that a crystalline ultra-thin silica film was obtained, but its structure was not known. DFT calculations with periodic boundary conditions were pivotal for selecting the right structure model from different suggestions. Comparison of calculated infrared and XPS spectra as well as simulated STM patterns showed that the film consists of a monolayer of corner sharing [SiO₄] tetrahedra as a two-dimensional (2D) network, with one corner oxygen bonded to the Mo atoms [1,2,9].
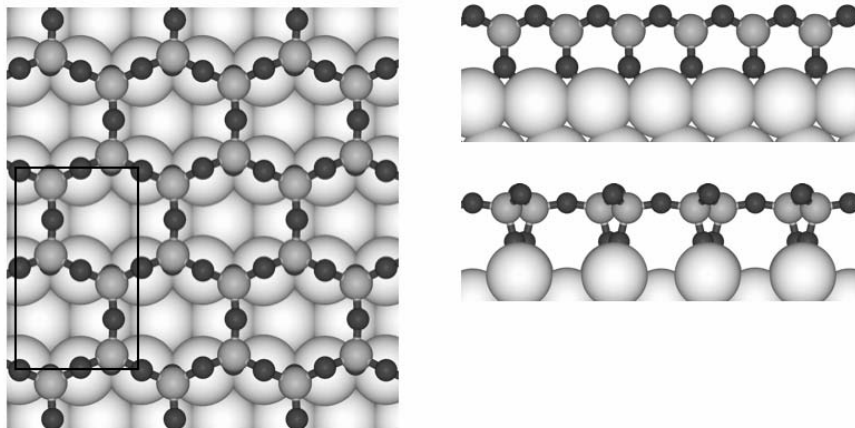
Figure 2. Hexagonal single layer silica film on Mo(112) [1,2]. The Si_4O_{10} unit cell is indicated.

The structure of this silica film resembles the sheet structure of monolayer silicates, and the film surface exposes Si-O-Si bonds similar to internal surfaces of microporous silica modifications. An alternative structure consisting of isolated SiO_4 tetrahedra that are bound with 4 Si-O-Mo bonds to the surface [10] could be clearly ruled out based on calculated IR spectra. The DFT calculations together with statistical mechanical stability calculations that account for the oxygen partial pressure also showed that the two-dimensional film is the most stable structure under all relevant experimental conditions. These calculations also predicted additional structures that would be stable under higher oxygen pressure and such a structure has indeed been identified by surface science techniques [11].

For vanadium oxides supported on silica and alumina oligomeric vanadia species with vanadyl groups and tetrahedral coordination of vanadium are found for low vanadium loadings [12]. Figure 3 shows monomeric and dimeric species that may exist on silica.
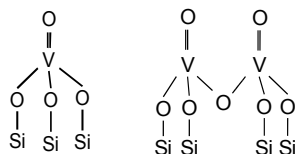

Figure 3. Monomeric and dimeric vanadia species on silica

For many years a Raman band around 950 cm^{-1} has been assigned to the V-O-V

bond and used to distinguish monomeric species that do not have this bond from dimeric and polymeric species. By combining quantum mechanical calculations for monomeric and dimeric species with Raman measurements of powder catalysts and IR absorption spectroscopy on UHV model catalysts it was possible to show that the absence of a band in the 950 cm^{-1} region does not indicate the absence of dimeric or polymeric species for supported VO_x/SiO_2 and VO_x/Al_2O_3 catalysts [3]. The V-O-V bands are expected below 850 cm^{-1} (were they are covered by bulk phonons of the support), while differences between the spectra of VO_x/SiO_2 and VO_x/Al_2O_3 in the 950 cm^{-1} range are due to V-O-Si/V-O-Al interphase modes and their coupling with bulk phonons

4. REACTIVITY OF SUPPORTED TRANSITION METAL OXIDE CATALYSTS

The mechanism of the C-H activation in the oxidation of methanol to formaldehyd and in oxidative dehydrogenation of propane by vanadium oxide catalysts is examined. The following question is frequently raised for supported transition metal oxides in general: Is the active site the transition metal oxo bond, e.g. V=O, or the interphase bond, e.g. V-O-Si. Calculations for the methanol oxidation on monomeric $O=V(OSi-)_3$ sites [13] showed that methanol chemisorbs onto the interphase V-O-Si, bond, but the rate-limiting oxidation occurs by hydrogen transfer to the metal oxo (V=O) bond. This is not in conflict with the finding [12] that the turnover frequency varies with the support, but not the V=O frequency. Specifically, the V=O frequency is a reactant property and such a correlation could exist, if at all, for early transition states only. It is also not in conflict with the observation that the transformation of $V={}^{18}O$ into $V={}^{16}O$ bonds is slower than the effective reaction rate [12]. In the mechanism resulting from the calculations the $V={}^{18}O$ oxygen atom ends up in the water produced and restoring the $V={}^{16}O$ bond during reoxidation of the catalyst is kinetically decoupled from the oxidation step (Mars-van Krevelen mechanism).

The oxidative dehydrogenation of propane also starts with adsorption of the hydrocarbon due to van der Waals forces. Among the suggested mechanisms for the initial C-H activation is addition of the C-H bond onto the vanadyl bond leading to VOH and V-R bonds [14]. We examined many possible pathways for the activation of the secondary C-H bond in propane at monomeric $O=V(OSi)_3$ sites and found that the initial activation step is hydrogen abstraction by the vanadyl bond leading to a biradical intermediate [15]. From this intermediate propene can be directly formed by a second hydrogen abstraction or a rebound mechanism can yield isopropanol strongly bound to the $V^{III}(OSi)_3$ surface site (Fig. 4).

Recently, Redfern et al. have suggested insertion of the vanadyl oxygen atom into the secondary C-H bond of propane as initial step which also leads to strongly adsorbed isopropanol [16]. The calculated barriers, 320 and 225 kJ/mol on the closed

shell singlet and triplet potential energy surfaces, respectively, are much higher than those shown in Figure 4. For the reaction of propane with a gas phase Mo_3O_9 cluster, H abstraction was also found to have a much lower barrier (135 kJ/mol) than direct O insertion into the C-H bond (218 kJ/mol) [17].
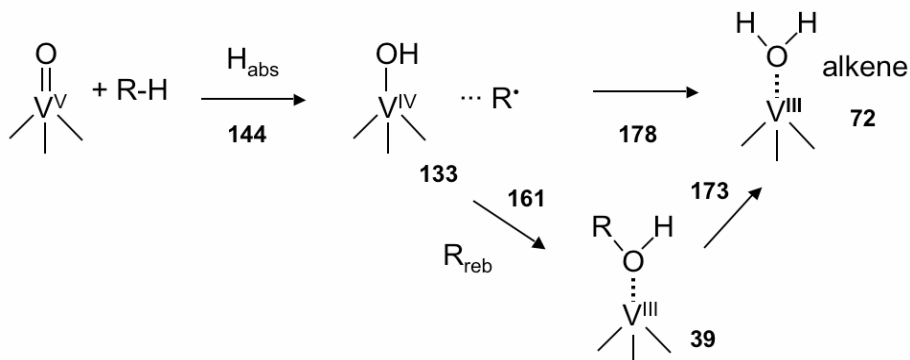

Figure 4. Two pathways for the oxidative dehydrogenation of propane on isolated monomeric vanadium oxide sites on silica [15]. Given are relative energies of intermediates and energy barriers at 0 K in kJ/mol.

The two consecutive hydrogen abstractions can also occur on two different vanadyl groups, either in two "cooperating" monomeric sites or in a dimeric site [18]. If only monomeric sites were present, the second hydrogen atom could be abstracted from the propyl radical by an unreacted $O=V(OSi)_3$ site elsewhere. As a result two $HOV^{IV}(d^1)$ sites are formed (Fig. 5) which is more favorable than formation of one $H_2O \cdot V^{III}(d^2)$ site. For dimeric sites, the reaction mechanism is the same, but the barriers are lower. Moreover, the lowering of the barriers is accompanied by a corresponding change of the reaction energies in accord with the Polaniy-Evans relation. Therefore, we can estimate the activity of oligomeric vanadium oxide species beyond dimers by calculating just reaction energies for the oxidative dehydrogenation of propane. We did this for models with one to four vanadyl groups and found a continuous decrease from dimeric to trimeric and tetrameric species [18].

This decrease of the energy barrier for the rate determining first hydrogen abstraction from monomeric to dimeric and further to polymeric species is the most important conclusion from the quantum mechanical calculations. This information cannot easily be obtained from experiments because supported catalysts with active species of uniform and controlled size cannot be prepared. The relative energies of the species with 0 to 4 vanadyl groups further indicate that there is no energetic preference for a particular size and that the distribution is rather statistical. This

means that with increasing vanadium loadings below a monolayer we may expect an increasing number of larger and, hence, more active species.
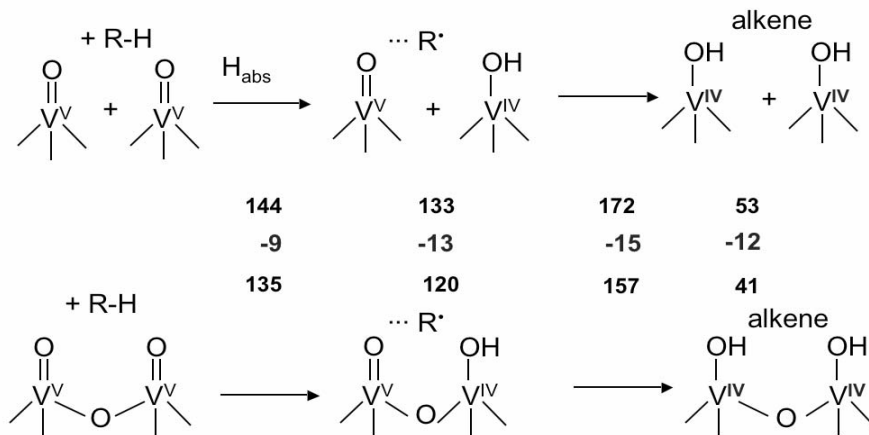

Figure 5: Comparison of reaction energies and energy barriers (kJ/mol) for two hydrogen abstractions from propane.

For comparison with experimental (apparent) activation energies, e.g. 122±20 kJ/mol [19] and 101±15 kJ/mol [20] we have to subtract the adsorption energy of propane (37±5 kJ/mol) from our calculated intrinsic barriers. This yields 139±8 kJ/mol for isolated monomeric sites and 103±5 kJ/mol for cooperating dimeric sites, which is in the right range.

We can go one step further and take the energy for dissociating the metal oxo bond as reactivity descriptor for transition metal oxides in oxidation catalysis [21]. Doing this we find, in agreement with observations [12,22], that the activity of crystalline V_2O_5 [23] is higher than that of vanadium oxide species supported on silica or alumina [21,24,25]. The high activity of crystalline V_2O_5 is due to formation of interlayer bonds on removal of the vanadyl oxygen atom which is not possible for oligomeric vanadia species or thin films on supports.

4   ACKNOWLEDGEMENT

5   REFERENCES

[1]   J. Weissenrieder, S. Kaya, J.-L. Lu, H.-J. Gao, S. Shaikhutdinov, H.-J. Freund, M. Sierka, T.K. Todorova, J. Sauer, Phys. Rev. Lett. 95 (2005) 0761031.

[2]   T.K. Todorova, M. Sierka, J. Sauer, S. Kaya, J. Weissenrieder, J.-L. Lu, H.-J. Gao, S. Shaikhutdinov, H.-J. Freund, Phys. Rev. B 73 (2005) 165404.

[3]   N. Magg, B. Immaraporn, J.B. Giorgi, T. Schroeder, M. Bäumer, J. Döbler, Z. Wu, E. Kondratenko, M. Cherian, M. Baerns, P.C. Stair, J. Sauer, H.-J. Freund, J. Catal. 226 (2004) 88.

[4]   C. Tuma, J. Sauer, Angew. Chem., Int. Ed. 44 (2005) 4769, Angew. Chem. 2005, 117, 4847.

[5]   C. Tuma, J. Sauer, Chem. Phys. Lett. 387 (2004) 388.

[6]   C. Tuma, J. Sauer, Phys. Chem. Chem. Phys. 8 (2006) 3955.

[7]   J. Hafner, L. Benco, T. Bucko, Top. Catal. 37 (2006) 41.

[8]   S. Grimme, J. Comput. Chem. 25 (2004) 1463.

[9]   L. Giordano, D. Ricci, G. Pacchioni, P. Ugliengo, Surf. Sci. 584 (2005) 225.

[10]   M.S. Chen, A.K. Santra, D.W. Goodman, Phys. Rev. B 69 (2004) 155404.

[11]   M. Sierka, T.K. Todorova, S. Kaya, D. Stacchiola, J. Weissenrieder, J. Lu, H. Gao, S. Shaikhutdinov, H.-J. Freund, J. Sauer, Chem. Phys. Lett. 424 (2006) 115.

[12]   B.M. Weckhuysen, D.E. Keller, Catal. Today 78 (2003) 25.

[13]   J. Döbler, M. Pritzsche, J. Sauer, J. Am. Chem. Soc. 127 (2005) 10861.

[14]   T. Blasco, J.M.L. Nieto, Appl. Catal. A 157 (1997) 117.

[15]   X. Rozanska, J. Sauer (2006). in preparation.

[16]   P.C. Redfern, P. Zapol, M. Sternberg, S.P. Adiga, S.A. Zygmunt, L.A. Curtiss, J. Phys. Chem. B 110 (2006) 8363.

[17]   G. Fu, X. Xu, X. Lu, H. Wan, J. Phys. Chem. B 109 (2005) 6416.

[18]   X. Rozanska, J. Sauer (2006). in preparation.

[19]   E. Kondratenko, M. Baerns (2006). Personal communication.

[20]   L. Owens, H.H. Kung, J. Catal. 144 (1993) 202.

[21]   J. Sauer, J. Döbler, Dalton Trans. 19 (2004) 3116.

[22]   I.E. Wachs, Catal. Today 100 (2005) 79.

[23]   M.V. Ganduglia-Pirovano, J. Sauer, Phys. Rev. B 70 (2004) 045422.

[24]   V. Brázdová, M.V. Ganduglia-Pirovano, J. Sauer, J. Phys. Chem. B 109 (2005) 23532.

[25]   T.K. Todorova, M.V. Ganduglia-Pirovano, J. Sauer, J. Phys. Chem. B 109 (2005) 23523.